Transformation and species identification of CuO nanoparticles in plant cells (Nicotiana tabacum)

Journal:	*Environmental Science: Nano*
Manuscript ID	EN-ART-07-2019-000781
Article Type:	Paper
Date Submitted by the Author:	11-Jul-2019
Complete List of Authors:	Dai, Yanhui; Jiangnan University Zhao, Jian; Ocean University of China, College of Environmental Science and Engineering Liu, Xiaoyun; Ocean University of China, College of Materials Science and Engineering Yu, Xiaoyu; Ocean University of China, College of Environmental Science and Engineering Jiang, Zhixiang; Qingdao University Bu, Yuyu; Xidian University, School of Microelectronics; Qingdao University of Science and Technology, School of Enviroment and Safty Eengineering Xu, Zefeng; Ocean University of China Wang, Zhenyu; Jiangnan University, Zhu, Xiaoshan; Tsinghua University, Xing, Baoshan; UMASS, Stockbridge School of Agriculture

SCHOLARONE™
Manuscripts

1
2
3
4
5
6
7
8
9
10
11
12
13
14
15
16
17
18
19
20
21
22
23
24
25
26
27
28
29
30
31
32
33
34
35
36
37
38
39
40
41
42
43
44
45
46
47
48
49
50
51
52
53
54
55
56
57
58
59
60

Environmental Significance

CuO nanoparticles (NPs) have raised concerns due to their applications in agriculture as fertilizers and pesticides. CuO NPs could undergo transformation in plant tissues (e.g., roots, shoots, leaves and seeds). However, the specific locations and reducing substances for the transformation are currently unknown. Our results showed that CuO NPs were transformed to Cu_2O, Cu_2S and Cu-acetate after incubation with plant cells. The transformation of CuO NPs initially occurred on cell walls. Galacturonic acid and cysteine are responsible for the formation of Cu_2O and Cu_2S NPs, respectively. After internalization, CuO NPs could also be transformed to Cu_2O and Cu_2S through interacting with protoplasts and mitochondria. These findings provide new insights for better understanding the transformation of metal-based NPs in living organisms and environments.

Transformation and species identification of CuO nanoparticles in plant cells (*Nicotiana tabacum*)

Yanhui Dai,[1,8] Jian Zhao,[2,3] Xiaoyun Liu,[4] Xiaoyu Yu,[2] Zhixiang Jiang,[5,8] Yuyu Bu,[6]

Zefeng Xu,[2] Zhenyu Wang,[1,*] Xiaoshan Zhu[7] and Baoshan Xing[8,*]

[1] Institute of Environmental Processes and Pollution Control, and School of Environmental and

Civil Engineering, Jiangnan University, Wuxi 214122, China

[2] College of Environmental Science and Engineering, and Ministry of Education Key Laboratory

of Marine Environment and Ecology, Ocean University of China, Qingdao 266100, China

[3] Laboratory for Marine Ecology and Environmental Science, Qingdao National Laboratory for

Marine Science and Technology, Qingdao 266237, China

[4] College of Materials Science and Engineering, Ocean University of China, Qingdao 266100,

China

[5] School of Environmental Science and Engineering, Qingdao University, Qingdao 266071, China

[6] Key Laboratory of Wide Band-Gap Semiconductor Materials and Devices, School of

Microelectronics, Xidian University, Xi'an 710071, China

[7] Graduate School at Shenzhen, Tsinghua University, Shenzhen 518055, China

[8] Stockbridge School of Agriculture, University of Massachusetts, Amherst, MA 01003, United

States

1
2
3
4   *Corresponding authors
5
6
7   Dr. Xing: bx@umass.edu; Dr. Wang: wang0628@jiangnan.edu.cn
8
9
10
11
12
13
14
15
16
17
18
19
20
21
22
23
24
25
26
27
28
29
30
31
32
33
34
35
36
37
38
39
40
41
42
43
44
45
46
47
48
49
50
51
52
53
54
55
56
57
58
59
60

Abstract

The transformation of CuO nanoparticles (NPs) during interacting with *Nicotiana tabacum* L. cv. Bright Yellow-2 (BY-2) cells was investigated in this study. CuO NPs were taken up, and transformed to Cu_2O, Cu_2S and Cu-acetate after incubation with plant cells for 12 h based on high resolution transmission electron microscope and X-ray absorption near-edge spectroscopy analysis. The transformation of CuO NPs initially occurred on cell walls with Cu_2O and Cu_2S being the main transformation products. Galacturonic acid as an important component of cell walls was mainly responsible for reducing CuO to Cu_2O and cysteine for the formation of Cu_2S. Cu^{2+} ions could not be transformed to any Cu-based particles (CuO, Cu_2O, or Cu_2S) on cell walls. After internalization, CuO NPs could also be transformed to Cu_2O and Cu_2S through interacting with protoplasts as well as mitochondria, confirming that CuO NPs were able to transform intracellularly. Moreover, Cu_2O NPs showed higher toxicity to plant cells as compared to CuO NPs with similar individual size, indicating that the transformation of CuO NPs enhanced their toxicity to plant cells. These findings could provide new insights for better understanding the transformation and fate of metal-based NPs in living organisms and environments.

Keywords:

BY-2 cells; Cu_2O; high resolution transmission electron microscope; extracellular polymeric substances; cell wall; toxicity

1. Introduction

Engineered nanoparticles (NPs) have been widely applied as fertilizers, pesticides, plant protection or pathogen detection in agriculture due to their outstanding properties.[1-3] It is reported that NPs could be taken into plants by roots and then translocated inside plants under root exposure.[4-7] After uptake by plants, original NPs such as CuO NPs could be transformed to other species (e.g., Cu_2O, Cu_2S).[5, 8, 9, 10] After transformation, their properties such as individual size and surface structure of NPs (e.g., CuO NPs) could be changed in plants, which may further affect their interaction with plants.[4] Plants are the primary producer in environmental ecosystems, and the interaction of NPs with plants can influence food safety and human health via food chain.[6] Therefore, it is important to understand the transformation processes of NPs in plants and the possible impact of these processes to phytotoxicity.

In terms of CuO NPs, it is reported that the transformation occurred in different tissues of plant, such as roots, shoots, leaves and seeds with different transformed products. For instance, CuO NPs were reduced to Cu_2S in a floating plant (*Eichhornia crassipes*) roots,[5] and Cu_2O and Cu_2S in maize (*Zea mays* L.) roots.[9] CuO (64%) and Cu(I)-S (36%) species were detected in the wheat shoots when the roots were exposed to CuO NPs.[8] Cu(II) in CuO NPs was reduced to Cu(I) and the proportion of Cu_2O was increased from roots to leaves of rice (*Oryza sativa* L.).[10] In addition, 6.0% of Cu was in the form of Cu_2O in the harvest seeds detected by X-ray absorption near-edge spectroscopy (XANES), when *Arabidopsis thaliana* was exposed to CuO NPs.[6]

Although CuO NPs could be transformed to other Cu species in different tissues, the specific locations for the transformation in plant cells are currently unknown. Transformation of CuO NPs relates to redox, sulfidation, and dissolution processes with the assistance of biomacromolecules in the biological systems.[11] It has been noted that the reducing substances (e.g., sugar, enzyme, organic acid) may relate to the redox and sulfidation processes of NPs.[9] In addition, CuO NPs are soluble, and can release dissolved ions.[12] It can be expected that the dissolution process also may induce further transformation of CuO NPs. Dimkpa et al. reported that Cu_2S and Cu(I)-cysteine products were formed in the shoots of Cu^{2+}-treated wheat indicated by XANES.[13] However, we recently found that CuO NPs were reduced to Cu_2O NPs as confirmed by high resolution transmission electron microscope (HRTEM) analysis, and the biotransformation was mainly following the NP internalization rather than the dissolved ions in algae.[14] These different results may be attributed to different species and culture conditions. However, the contribution of different substances on CuO NP transformation, and the formation of CuO NPs (or Cu(I) species) from the dissolved Cu^{2+} ions in plant are still unclear.

Additionally, transformation may further alter the toxicity of CuO NPs. It is observed that the transformed CuS NPs showed significantly lower toxicity than original CuO NPs in murine macrophages,[15] while showing higher toxicity in Japanese medaka (*Oryzias latipes*).[16] Although these studies yielded inconsistent results, it can be deduced that the toxicity of CuO NPs did change after transformation. It is reported that Cu_2O NPs exhibited higher toxicity to bovine aortic

endothelial cells than CuO NPs at concentrations higher than 10 μg/mL due to the

oxidation of Cu^+ to Cu^{2+}, which caused the oxidative stresses to the mitochondria and

thus resulted in the autophagy of the endothelial cells.[17] However, the toxicity of

Cu(I) species transformed from CuO NPs in plants or plant cells is currently

unknown. Therefore, we hypothesized that CuO NPs can be reduced to Cu(I) species

by reducing substances such as GlaA-containing polysaccharides, the primary

reducing sugar in plant cell walls,[18] and the transformed Cu species may alter the

toxicity to plant cells. In the present work, we chose plant cells, the basic unit of

plants, to investigate the transformation of CuO NPs at cellular level. The main aims

of this study were to (1) localize the transformation sites of CuO NPs in plant cells;

(2) probe the reducing substances that are responsible for CuO NP transformation;

and (3) explore the effect of CuO NP transformation on the toxicity to plant cells. The

information provided in the present work will be important for understanding the

transformation and fate of metal-based NPs in plants.

2. Materials and Methods

2.1 Characterization of CuO NPs and Cu_2O NPs

CuO NPs were purchased from Sigma-Aldrich, and Cu_2O NPs were obtained

from Beijing Dk Nano technology Co., LTD. The size, morphology and crystal plane

of individual NPs were observed by HRTEM (JEM-2100, JEOL, Japan). Briefly, CuO

NPs were suspended in ethanol and 1/2 MS medium (Table S1), respectively, and the

Cu_2O NPs were suspended in ethanol by sonication (100 W, 40 kHz) for 30 min.

Then, a drop of suspension was added onto a nickel grid for the following TEM

observation. X-ray diffraction (XRD, Bruker D8 ADVANCE, Germany) was used to characterize the crystal structure of the CuO and Cu$_2$O NPs. The zeta potentials and hydrodynamic diameters of CuO NPs (12 mg/L) and Cu$_2$O NPs (10.8 mg/L) in ultrapure water (pH 5.8) and 1/2 MS medium (pH 5.8) were determined by a Zetasizer (Nano-ZS90, Malvern Instruments, Ltd., UK). For the dissolution of Cu$_2$O NPs, after incubation for 0, 0.5, 2, 6, 12, 24, and 36 h, the suspended Cu$_2$O NPs in 1/2 MS medium (10.78 mg/L) were filtered through a 0.22-μm membrane filter after centrifugation twice at 10,000 rpm for 30 min,[12] and then determined with inductively coupled plasma mass spectrometer (ICP-MS) (Perkin Elmer NexION 350X, Shelton, USA). Dissolution of CuO NPs (12 mg/L) was determined by following the same approach in our previous work.[12]

2.2 CuO NP distribution and transformation as observed by TEM

The morphology and distribution of CuO NPs in plant cells were analyzed by HRTEM. *Nicotiana tabacum* L. cv. Bright Yellow-2 (BY-2) cells (5×10^5 cells/mL) were provided from the College of Life Sciences and Oceanography, Shenzhen University. The 24 h median effective concentration (EC$_{50}$) of CuO NPs to BY-2 cells was 12 mg/L.[12] Thus, the concentration of CuO NPs used in this study was selected at 12 mg/L. The un-exposed BY-2 cells and CuO NP-exposed (12 mg/L, 20 mL, 12 h) cells (5×10^5 cells/mL) were washed three times with 20 mM ethylene diamine tetraacetic acid (EDTA) and phosphate buffer (PBS, 20 mM, pH 7.2), respectively.[12] After centrifugation (1,000 ×g, 10 min), the collected cells were further fixed in 3% glutaraldehyde for 12 h. The cells were then washed with PBS three times and

post-fixed in 1% osmium tetraoxide. After fixation, the cells were dehydrated in acetone, and embedded in EPON812 resin. The ultrathin sections were made for HRTEM observation along with energy dispersive spectroscopy (EDS, INCA100, Oxfordshire, UK).

2.3 XANES analysis of Cu species after CuO NP exposure

XANES was used to analyze the Cu species of CuO NPs after interacting with whole cells and cell walls. For whole cells, after exposure to CuO NPs (12 mg/L) over 12 h, plant cells (5×10^5 cells/mL) were collected, washed with EDTA and PBS, freeze- dried (FD5-series, SIM, USA), and then ground into fine powders for XANES analysis. For cell walls, they were firstly extracted from cells that were pre-treated with CuO NPs (12 mg/L, 12 h) according to the methods of Zhong and Lauchli as follows.[19] Briefly, cells were firstly washed with EDTA and PBS after exposing to CuO NPs (12 mg/L, 12 h), added into ice-cold ethanol solution (95%, v/v) to dehydration, and ground to powder in the mortar containing liquid nitrogen. These powders were added ice-cold 75% ethanol to sonicate (120 W) for 2 min, and cultured in ice-bath for 20 min. The suspensions were then centrifuged for 10 min (1,000 ×g). The pellets at the bottom were washed with ice-cold acetone, methanol-chloroform mixture (1:1, v/v), methanol and ultrapure water for 20 min, respectively. Each time, the supernatants were discarded after centrifugation. The finally collected pellets were the extracted cell walls, which were freeze-dried and ground to powder for further XANES analysis. In this experiment, the cells exposed to CuO NPs (12 mg/L, 12 h)

were defined as CE. The cell walls extracted from CuO NP-exposed (12 mg/L, 12 h) cells were denoted as CW.

XANES data at the K-edge of Cu (8979 eV) were collected at the beamline 14W1 at Shanghai Synchrotron Radiation Facility (SSRF, Shanghai, China). The spectra of the following commercial Cu reference standards (CuSO$_4$, CuS, Cu$_2$(OH)PO$_4$, Cu-citrate, CuO NPs, Cu-acetate, Cu$_2$O, Cu$_2$S) in their solid powder forms were collected using X-ray transmission mode. However, the whole cells after CuO NP exposure and the cell walls extracted from CuO NP-exposed cells were collected from fluorescence mode by Lytle detector because of the low Cu concentration.[20] XANES data processing and linear combination fitting (LCF) were analyzed by ATHENA software.[21]

2.4 Transformation of CuO NPs and Cu^{2+} in the presence of cell walls or extracellular polymeric substances

Plant cells were treated with CuO NPs (12 mg/L) or Cu^{2+} (0.8 mg/L) for 12 h. Cu^{2+} at 0.8 mg/L was selected based on the dissolution of CuO NPs (12 mg/L) in the medium from our previous study.[12] After exposure, cells were washed with EDTA and PBS for several times, and then cell walls were extracted as mentioned in 2.3 and suspended in ultrapure water for HRTEM observation. These cell walls were defined as "cell walls from CuO NP-exposed cells". In addition, the cell walls extracted from untreated plant cells were exposed to CuO NPs (12 mg/L) or Cu^{2+} (0.8 mg/L) over 12 h for further observation with HRTEM. These cell walls were named as "CuO NP-exposed cell walls". In addition, plant cells were cultured in the medium for 3

days, and filtered by a sterilized 18-μm stainless steel sieve. The filtrate was considered as extracellular polymeric substances (EPS).[22] The EPS were further reacted with CuO NPs (12 mg/L) or Cu^{2+} (0.8 mg/L) for 12 h. The solutions were then dropped onto the nickel grid for further HRTEM observation.

2.5 Transformation of CuO NPs during interaction with cell wall components

Galacturonic acid (GalA) was used to investigate the role of reducing sugar in the transformation of CuO NPs. The actual GalA contents of cell walls extracted from the un-exposed and CuO NP-exposed cells were measured. Briefly, the cell walls of un-exposed cells and CuO NP-exposed (12 mg/L, 12 h) cells were extracted by following the approach above. Then, the extracted cell walls of un-exposed and CuO NP-exposed cells were hydrolysed with 2 M trifluoroacetic acid (TFA) at 121 °C for 1 h. The suspension containing cell walls was sealed and filled with N_2 rapidly. After cooled down to room temperature, the cell wall solution was concentrated to dryness in a rotary evaporator. The residues were extracted with methanol, and evaporated to dryness again. The final extracted GalA was diluted with ultrapure water, and sealed in -20 °C under N_2 for further determination. GalA content was determined according the method of Blumenkrantz and Asboe-Hansen at 520 nm by Microplate Reader (Thermo, USA).[23] Uronic acid accounted for 30.8% of cell walls in tobacco mesophyll,[24] and changed with different growth stages.[18] Consequently, the final content of GlaA was chosen as 40% of cell walls. In this study, the yield of cell walls was 50 mg as extracted from 4 g fresh cells in 100 mL medium, which was slightly higher than that reported by a previous study (about 1 g cell walls from 100 g fresh

cells).[25] Therefore, the final exposure concentrations of GlaA and CuO NPs were selected as 200 and 12 mg/L, respectively. The commercial GlaA (Beijing Solarbio Science & Technology Co., Ltd., Beijing, China) was then used for the CuO NP transformation investigation. CuO NPs (12 mg/L) were added into the GlaA solution prepared in ultrapure water, and incubated for 12 h at 25 °C under N_2 in dark. One drop of GlaA-treated CuO NP samples was placed onto the nickel grid for HRTEM observation. In addition, the above sample (named "CuO NPs+GalA") was freeze-dried for Fourier transform infrared spectroscopy (FTIR, Spectrum 100, Perkin-Elmer Inc., USA) analysis.

Moreover, L-cysteine was used to represent the S-containing proteins in cell walls. The protein content was 18 mg per g tobacco cell walls,[26] and thus the concentration of L-cysteine was calculated at 9 mg/L. L-cysteine (Sinopharm Chemical Reagent Co., Ltd., Shanghai, China) and CuO NPs (12 mg/L) were thoroughly mixed in ultrapure water, and incubated for 12 h at 25 °C under N_2 in dark. Then, one drop of the mixed solution was dropped onto the nickel grid for HRTEM observation.

2.6 Transformation of CuO NPs during incubation with protoplast and mitochondria

The protoplasts were isolated as described by Shepard and Totten with slight modification.[27] Briefly, plant cells were incubated with mixed enzyme solution (3% cellulase R10, 0.4% macerozyme R10, 400 mM mannitol, 20 mM MES and 10 mM $CaCl_2$, pH 5.8) in dark for 6 h in a shaker (60 rpm/min, 24°C). Then, the cells were

filtered by a sterilized 18-μm stainless steel sieve, and incubated with sucrose solution (25% w/v). The protoplasts were collected by centrifugation at 800 ×g for 5 min, and purified by W5 medium (154 mM NaCl, 5 mM glucose, 0.03% MES, 5 mM KCl, 125 mM $CaCl_2$, pH 5.8) for 3 times. The protoplasts were broken under sonication (120 W) for 2 min and then filled with N_2 immediately for 5 min for further study. Mitochondria were isolated by suspending the extracted protoplasts in mitochondrial wash buffer (440 mM sucrose, 50 mM Tris HCl, 20 mM EDTA, pH 8.0), and collected by centrifugation at 16,000 ×g for 20 min at 4 °C.[28] The obtained protoplasts and mitochondria were incubated with CuO NPs (12 mg/L) for 12 h under N_2. After incubation, the protoplasts and mitochondria were made into ultrathin sections, and observed by HRTEM.

2.7 Cell viability upon exposure to CuO and Cu₂O NPs

Cell viability was determined by the 2, 3, 5 - triphenyltetrazolium chloride (TTC, Sigma) method. Briefly, cells ($5×10^5$ cells/mL) were incubated with CuO NPs (12 mg/L) or Cu_2O NPs (10.8 mg/L) for 2, 4, 8, 16 and 24 h in 24-well plates in 1/2 MS medium at 25 °C. TTC (0.3%, v/v) was added into the culture after removing the supernatant by centrifugation (1,000 ×g, 10 min). The obtained cells were cultured for 10 h, and centrifuged at 1,000 ×g for 10 min to remove the supernatant. After adding 95% ethanol into the culture, the cultures were heated at 60 °C for 15 min. The optical densities at 485 nm were determined by a Microplate Reader (Thermo, USA).

2.8 Statistical analysis

The mean value ± standard deviation (SD) of triplicates for each treatment was

calculated. One-way analysis of variance (ANOVA) by Tukey test using the SPSS

18.0 statistical software, was applied to evaluate the significant differences. The $p <$

0.05 was considered as significant difference.

3. Results and Discussion

3.1 Characterization of NPs

The TEM images in Figure 1A show that CuO NPs were spherical particles and

the size of individual NPs was around 40-50 nm. In addition, CuO NPs were

composed of pure polycrystal CuO particles (1-2 nm) as revealed by HRTEM (Figure

S1A). CuO NPs suspended in 1/2 MS medium formed aggregates (Figure S1B). The

1/2 MS medium did not contribute to any transformation of CuO NPs (Figure S1C).

The size of Cu_2O NPs was 50 nm (Figure 1B). XRD revealed that CuO NPs showed

crystalline structure, and did not contain any Cu_2O in the samples. The main

diffraction peaks were corresponded to (11-1) and (111) crystal faces for CuO NPs

(Figure 1C). Cu_2O NPs were composed of Cu_2O crystals, and no impurities (e.g.,

CuO) were detected in the Cu_2O NPs. The main crystal faces for Cu_2O NPs were

(111) and (200) (Figure 1D). Both CuO NPs and Cu_2O NPs were negatively charged

in both ultrapure water and 1/2 MS medium (Table S2). The hydrodynamic diameters

of CuO NPs and Cu_2O NPs in 1/2 MS medium were 557.5 ± 28.60 and 570 ± 31.45

nm, respectively. This indicated that CuO NPs and Cu_2O NPs aggregated in both 1/2

MS medium and ultrapure water (Table S2).

3.2 Speciation of Cu in plant cells after CuO NP exposure

Black dots were found on the cell wall surface (Figure 2B), inside the cell wall

(space between cell wall and plasma membrane) (Figure 2C, 2D) and in the vacuole (Figure 2A). All the detected black dots contained Cu (ranged from 2.44 to 4.95%, weight percentage) as confirmed by EDS (Figure S2), suggesting that these black dots were Cu-containing particles. From HRTEM analysis, it is clear that the particles on the cell wall surface consisted of CuO and Cu_2O (Figure 2E), and the sizes (1-2 nm) were the same as the polycrystal CuO particle sizes (Figrue S1A). The crystal planes were (111), (110) and (11-2) for CuO, and (200) for Cu_2O (Table S3). In addition, CuO, Cu_2O and Cu_2S were identified inside the cell wall (space between cell wall and plasma membrane) and vacuole (Figure 2F, 2G). Inside the cell walls, the crystal planes of CuO were mainly (11-2) and (110). The crystal spacings were calculated to be 0.296 nm and 0.33 nm, corresponding to Cu_2O (110) and Cu_2S (002), respectively (Table S3). In the vacuole, the crystal planes of CuO were (11-2), (20-2), (002), and (110). The crystal planes of Cu_2O and Cu_2S in vacuole were the same as that inside the cell walls. It is noted that the pristine CuO NPs did not contain Cu_2O or Cu_2S as detected by HRTEM and XRD (Figure S1, Figure 1). However, no elemental Cu can be detected in the un-exposed cells (Figure S3). Therefore, the transformation of CuO should firstly take place along interacting with plant cell walls. In addition to the formation of Cu_2O, CuO NPs were transformed to Cu_2S during CuO NP internalization.

XANES was used to further identify the Cu species in CuO NP-exposed plant cells and cell walls. Normalized Cu K-edge XANES spectra and the percentage of Cu-species of CE (cells after exposed to 12 mg/L CuO NPs for 12 h) and CW (cell

walls extracted from CuO NP-exposed cells) are shown in Figure 3. Fitting spectra of

CE and CW display a mixture of CuO NPs, Cu_2S, Cu_2O and Cu-acetate. In CE group,

Cu species were mainly CuO (34%), Cu_2S (21%), Cu_2O (32%), and Cu-acetate

(13%). In CW group, the percentages of CuO (42%) and Cu-acetate (28%) were

higher than those in CE group, while the proportions of Cu_2O (15%) and Cu_2S (15%)

in CW were slightly lower. In the un-exposed cells, Cu species were not detected by

XANES because of detection limit, suggesting that the Cu background in plant cells

had no influence on the analysis of Cu species in CuO NP-exposed cells. All these

results indicate that CuO NPs were transformed into Cu_2O, Cu_2S, and Cu-acetate on

the cell walls and in the cells. Additionally, CuO NPs were primarily reduced to Cu(I)

species (e.g., Cu_2O, Cu_2S) on the cell walls.

Cell wall was the initial location for the interaction of CuO NPs with plant cells.

We thus further investigated the transformation of CuO NPs by cell walls and EPS.

CuO NPs were transformed to Cu_2O and Cu_2S in both "CuO NP exposed-cell walls"

and "cell walls extracted from CuO NP-exposed cells" treatments (Figure 4D, 4E).

The crystal planes of CuO, Cu_2O and Cu_2S are listed in Table S4. However, after 12-h

incubation, the transformation of CuO NPs was not found in the EPS treatment

(Figure 4F). Combining these TEM (Figure 2) and XANES (Figure 3) results, it can

be concluded that partial Cu(II) in CuO NPs was transformed to Cu(I) firstly on cell

walls. The detected Cu-species were hypothesized to be formed by interacting of CuO

NPs with cell wall components (e.g., polygalacturonic acid or other reducing

substances), which was further discussed in the next section.

3.3 Transformation of CuO NPs during interacting with cell wall components

Spielman-Sun et al. reported that CuO NPs could be transformed to Cu(II)-O-R species due to the bound of Cu ions to polygalacturonic acid in plant cell walls.[4] However, the specific reducing agents related to the transformation of CuO NPs to Cu(I) by cell walls were currently unknown. Plant cell walls were made up of carbohydrates, proteins, and aromatic compounds.[18] Thus, functional groups in the cell walls such as carboxylic, amino, sulfhydryl, and hydroxy groups are major sources of adsorption/binding sites for metal ions.[29] GlaA-containing polysaccharides are the major reducing sugar in plant cell walls.[18] Therefore, CuO NPs were treated with GalA to investigate the transformation mechanisms by cell walls. As shown in Figure 5B, the formation of Cu_2O was observed. The crystal spacings of CuO were 0.141 and 0.233 nm which were in accordance with (31-1) and (111) crystal planes, respectively. The crystal spacings of Cu_2O (221) and (200) were 0.143 and 0.218 nm, respectively. We then further studied the content of GalA in the cell walls under the exposure of CuO NPs (12 mg/L) for 12 h, which was significantly increased (Figure 5C). The content of GalA in cell walls extracted from CuO NP-exposed cells increased by 61.5% compared with that from un-exposed cells. Similarly, Miao et al. reported that aldehyde containing substances was increased when algae exposed to silver NPs.[30] When exposed to Cd(II), the uronic acid contents in *Synechocystis* sp. BASO671 increased by 14.8%, and the GalA proportion of EPS increased from 0.08% in control group to 2.6% in Cd(II) group.[31] GalA is a vital fungal glucan elicitor, playing an important role in plant defensive responses. The increased content

of GalA may be due to the cell defense against adversity stress (CuO NP exposure). The FTIR data showed the changed groups after GalA incubated with CuO NPs (Figure S4). A new band appeared at 2559 cm^{-1} in the "CuO NPs+GalA" treatment, which was assigned to the OH stretching of COOH dimers,[32] suggesting the formation of COOH (e.g., formic acid). The strong vibration bands at 1726 cm^{-1} and 1710 cm^{-1} of GalA were related to the C=O stretching vibration of COOH,[32] and shifted to 1622 cm^{-1} of "CuO NPs+GalA". These bands changed in intensity and position, which were possibly due to the binding of GalA with copper ions or CuO NPs. The band (624 cm^{-1}) in "CuO NPs+GalA" indicated the presence of Cu_2O.[33] However, the peak at 538 cm^{-1} was for CuO.[34] Given that neither GalA treatment nor CuO NPs showed Cu_2O band, it can be concluded that CuO was transformed to Cu_2O with the assistance of GalA. Previous study showed that the ring of the GalA was opened and the aldehydic group was formed during the binding and redox process.[35] It was possible that the formed aldehyde groups were oxidized to carboxyl groups. Meanwhile, CuO was reduced into Cu_2O. Panigrahi et al. reported that reducing sugars were used as reducing agent for the synthesis of metal NPs (e.g., gold, silver).[36] In the GalA-iron system, Fe (III) was reduced to Fe (II) by GalA, while the aldehydic end group and the final carbon group of GalA were oxidized to formic acid and carboxylic forms, respectively.[35] Also, Branca et al. reported that D-Galacturonic acid transformed chromium (VI) into water-soluble chromium (V) species.[37]

In addition, Cu_2S was also formed during the interaction of CuO NPs with cell walls. Cysteine was used to investigate the contribution of sulfhydryl groups on the

reduction of Cu(II) to Cu(I). After incubated with L-cysteine for 12 h, CuO NPs were transformed to Cu_2S with the crystal planes of Cu_2S (-223) and (213) as determined by HRTEM (Figure 5D). The formation of Cu_2S may be ascribed to the following processes: CuO was reduced to Cu_2O, and then transformed to Cu_2S directly on the CuO surface; or the formed Cu_2O directly reacted with sulfide (e.g., cysteine).[38, 39] Although only Cu_2S particles were found during the interaction of CuO NPs with L-cysteine, Cu_2O and Cu_2S particles did occur on the cell walls and in cells (Figure 2). These results indicated that cysteine was primarily responsible for the formation of Cu_2S.

In addition, previous study reported that Cu^{2+} ions could form Cu-based NPs during interacting with plants. Cu^0 NPs were detected in the rhizosphere of *Phragmites australis* and *Iris pseudoacorus* when treated with Cu ions.[40] *Arachis hypogaea* L. leaf could reduce Cu^{2+} to Cu_2O NPs with aldehyde groups in the reducing sugars as reducing agents.[33] In the present work, it is possible that the detected Cu_2O or Cu_2S NPs in plant cells were formed from the Cu^{2+} ions released by CuO NPs. Therefore, Cu^{2+} ions were directly incubated with the extracted cell walls or EPS. It is shown that no black particle was found from TEM images when Cu^{2+} ions were interacted with extracted cell walls or EPS for 12 h (Figure S5). This suggested that Cu^{2+} ions cannot be formed into CuO, Cu_2O or Cu_2S particles along interacting with cell walls or EPS in the present work. Therefore, CuO, Cu_2O or Cu_2S particles in the cell walls were formed from the transformation of CuO NPs rather than the released Cu^{2+} ions. This finding was supported by the results that Cu^{2+} did
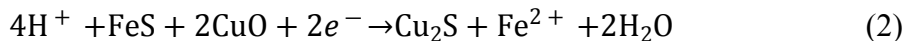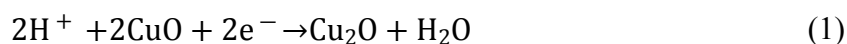
not contribute to the formation of Cu_2O NPs in algae.[14] Cu^{2+} ions dissolved from CuO NPs were mainly in the form of Cu complexes by binding with organic ligands (e.g., cysteine) in plant cells.[13]

3.4 Intracellular transformation of CuO NPs

The pore size of cell wall is about 5-20 nm,[41] which limits cellular internalization of exogenous particles such as CuO NPs. As shown in Figure S1, individual CuO NPs were composed of particles at 1-2 nm. The sizes of these particles were less than the pore size of cell walls, which made it possible for them to enter the cells. Besides, it is reported that the uptake of NPs by endocytosis was an important way of plant cells.[12] Previous study suggested that trace metals were taken up by cells which formed metal-based complexes on the plasmalemma.[29] Once entering cells, there were also redox substances inside the cells. Thus, in the following study, the isolated protoplasts were incubated with CuO NPs for 12 h to investigate the redox reaction of CuO NPs inside cells. As shown by HRTEM, CuO NPs were reduced into Cu_2O (Figure 6B) and Cu_2S after incubation with the isolated protoplasts (Figure 6C). The crystal and the corresponding crystal spacings were summarized in Table S5.

The intracellular proteins and organic acids containing sulfhydryl groups may account for the formation of Cu_2S inside cells. In addition, mitochondria were the main organelle played vital roles in cell redox homeostasis.[42] The isolated mitochondria were used for CuO NP transformation to identify their role in the reduction of CuO NPs. After incubating with mitochondria for 12 h, CuO NPs were also reduced into Cu_2O and Cu_2S (Figure 6E, 6F). It is reported that the reduction of

Cu^{2+} in the copper complexes was influenced by hydrated electron, radical or ionic species generated by energetic electrons or the ligands.[43] In our previous study, CuO NPs inhibited the activity of NADH dehydrogenase complex (complex I) and cytochrome *c* reductase complex (complex III) in mitochondria, blocked the transfer of electrons.[12] Complex I contains FeS centers. The inhibited activity of complex I led to the accumulation of H^+ and FeS centers. CuO thus could interact with H^+ and FeS to produce Cu_2O and Cu_2S. Also, the inhibited activity of complex III could result in the accumulation of H^+, leading to a stronger acidic environment which may contribute to the dissolution of CuO NPs. The chemical reactions are shown in equations (1) and (2) as follows.

$$2H^+ + 2CuO + 2e^- \rightarrow Cu_2O + H_2O \qquad (1)$$

$$4H^+ + FeS + 2CuO + 2e^- \rightarrow Cu_2S + Fe^{2+} + 2H_2O \qquad (2)$$

After transformation, the toxicity of CuO NPs may be changed. The toxicity of CuO and Cu_2O NPs represented as Cu(II) and Cu(I) species to plant cells were thus investigated, and the cell viabilities are shown in Figure S6. At the equivalent weight of Cu, Cu_2O NPs showed significantly higher toxicity to plant cells than CuO NPs for all the exposure times (0-24 h). After exposure for 2 h, cell viability of Cu_2O NPs was sharply reduced to 5.2% compared with control, while that of CuO NPs was 79.0%. Over 24 h, cell viability was still 56% for CuO NPs. Toxicity of these two NPs were originated from both particles and released ions. Our previous study showed that Cu^{2+} concentration released from CuO NPs was just 0.73 mg/L after incubation for 36 h.[12] The concentration of Cu ions released from Cu_2O NPs was 1.55 mg/L after 0.5 h,

which was much higher than that from CuO NPs (Figure S7). Both the zeta potentials and hydrodynamic diameters did not show any significant difference between CuO NPs and Cu_2O NPs in 1/2 MS medium (Table S2). Therefore, the higher dissolution of Cu_2O NPs may be the main reason for the observed higher toxicity than CuO NPs. Indeed, Seo et al. found that Cu_2O was much more toxic to endothelial cells than CuO, and the oxidation process of Cu^+ ions to Cu^{2+} ions was responsible for the oxidative stress and consequent cell death.[17] Given the higher toxicity of Cu_2O NPs, the transformation of Cu (II) in CuO NPs to Cu(I) may enhance the toxicity. Cu is an essential element for plant, but is toxic in excess. Part of Cu(II) ions needs to transform to Cu(I) before entry into cells and inside cells, since CRT/COPT families (high affinity transporters) are only able to recognize Cu(I) and then donate Cu(I) to chaperones.[44] This may explain why Cu(II) was transformed to Cu(I) by plant cells. Plants and microbes surrounding the plant roots could supply reducing environments by producing reducing substances.[9, 45] In addition, non-aerated soil or wetland are typical reducing environments.[11] Consequently, NPs could undergo transformation in the natural environment, and the toxicity of the transformed product may be different from the original NPs.

4. Conclusions

In the present study, it is observed that CuO NPs underwent reduction and sulfidation when interacting with plant cells. The transformed products were detected as Cu_2O, Cu_2S and Cu-acetate. The transformation of CuO NPs firstly occurred on plant cell walls, associated with reducing sugars (e.g., GlaA) and sulfur-containing

proteins (e.g., L-cysteine). It should be noted that the dissolved Cu^{2+} did not form any Cu-containing particles on plant cell walls and/or through EPS. The transformation of CuO NPs also occurred intracellularly, and protoplast and mitochondria were the main locations for CuO NP transformation. When exposed to equivalent weight of Cu, Cu_2O NPs exhibited higher toxicity than CuO NPs, implying that the transformation may elevate the toxicity upon CuO NP exposure. Reductive compounds are ubiquitous in the organisms or environment. Given that transformation may occur in organisms, this could be a possible mechanism for the high toxicity of CuO NPs to different organisms. Moreover, the transformation of CuO NPs could also occur in environments (e.g., benthic environments). Once released into environment, comprehensive understandings on the toxicity of transformed NPs should be paid much more attention.

Supplementary Information.

Seven figures and five tables. This material is available free of charge via the Internet at http://pubs.rsc.org/.

Conflicts of interest

The authors declare no conflict of interest.

Acknowledgements

References:

1. N. R. Scott, H. Chen and H. Cui, Nanotechnology applications and implications of agrochemicals toward sustainable agriculture and food systems, *J. Agric. Food Chem.*, 2018, **66**, 6451-6456.

2. A. A. Malandrakis, N. Kavroulakis and C. V. Chrysikopoulos, Use of copper, silver and zinc nanoparticles against foliar and soil-borne plant pathogens, *Sci. Total Environ.*, 2019, **670**, 292-299.

3. L. R. Khot, S. Sankaran, J. M. Maja, R. Ehsani and E. W. Schuster, Applications of nanomaterials in agricultural production and crop protection: a review, *Crop prot.*, 2012, **35**, 64-70.

4. E. Spielman-Sun, E. Lombi, E. Donner, A. Avellan, B. Etschmann, D. L. Howard and G. V. Lowry, Temporal evolution of copper distribution and speciation in roots of *Triticum aestivum* exposed to CuO, Cu $(OH)_2$, and CuS nanoparticles, *Environ. Sci. Technol.*, 2018, **52**, 9777-9784.

5. J. Zhao, W. Ren, Y. Dai, L. Liu, Z. Wang, X. Yu, J. Zhang, X. Wang and B. Xing, Uptake, distribution and transformation of CuO NPs in a floating plant *Eichhornia crassipes* and related stomatal responses, *Environ. Sci. Technol.*, 2017, **51**, 7686-7695.

6. Z. Wang, L. Xu, J. Zhao, X. Wang, J. C. White and B. Xing, CuO nanoparticle interaction with *Arabidopsis thaliana*: Toxicity, parent-progeny transfer, and gene

expression, *Environ. Sci. Technol.*, 2016, **50**, 6008-6016.

7. C. Peng, C. Xu, Q. Liu, L. Sun, Y. Luo and J. Shi, Fate and transformation of CuO nanoparticles in the soil-rice system during the life cycle of rice plants, *Environ. Sci. Technol.*, 2017, **51**, 4907-4917.

8. C. O. Dimkpa, J. E. McLean, D. E. Latta, E. Manangón, D. W. Britt, W. P. Johnson, M. I. Boyanov and A. J. Anderson, CuO and ZnO nanoparticles: phytotoxicity, metal speciation, and induction of oxidative stress in sand-grown wheat, *J. Nanopart. Res.*, 2012, **14**, 1125.

9. Z. Wang, X. Xie, J. Zhao, X. Liu, W. Feng, J. C. White and B. Xing, Xylem- and phloem-based transport of CuO nanoparticles in maize (*Zea mays* L.), *Environ. Sci. Technol.*, 2012, **46**, 4434-4441.

10. C. Peng, D. Duan, C. Xu, Y. Chen, L. Sun, H. Zhang, X. Yuan, L. Zheng, Y. Yang, J. Yang, X. Zhen, Y. Chen and J. Shi, Translocation and biotransformation of CuO nanoparticles in rice (*Oryza sativa* L.) plants, *Environ. Pollut.*, 2015, **197**, 99-107.

11. G. V. Lowry, K. B. Gregory, S. C. Apte and J. R. Lead, Transformations of nanomaterials in the environment, *Environ. Sci. Technol.*, 2012, **46**, 6893-6899.

12. Y. Dai, Z. Wang, J. Zhao, L. Xu, L. Xu, X. Yu, Y. Wei and B. Xing, Interaction of CuO nanoparticles with plant cells: internalization, oxidative stress, electron transport chain disruption, and toxicogenomic responses, *Environ. Sci.: Nano*, 2018, **5**, 2269-2281.

13. C. O. Dimkpa, D. E. Latta, J. E. McLean, D. W. Britt, M. I. Boyanov and A. J.

Anderson, Fate of CuO and ZnO nano- and microparticles in the plant environment, *Environ. Sci. Technol.*, 2013, **47**, 4734-4742.

14. J. Zhao, X. Cao, X. Liu, Z. Wang, C. Zhang, J. C. White and B. Xing, Interactions of CuO nanoparticles with the algae *Chlorella pyrenoidosa*: adhesion, uptake, and toxicity, *Nanotoxicology*, 2016, **10**, 1297-1305.

15. Z. Wang, A. Von Dem Bussche, P. K. Kabadi, A. B. Kane and R. H. Hurt, Biological and environmental transformations of copper-based nanomaterials, *ACS Nano*, 2013, **7**, 8715-8727.

16. L. Li, L. Hu, Q. Zhou, C. Huang, Y. Wang, C. Sun and G. Jiang, Sulfidation as a natural antidote to metallic nanoparticles is overestimated: CuO sulfidation yields CuS nanoparticles with increased toxicity in medaka (*Oryzias latipes*) embryos, *Environ. Sci. Technol.*, 2015, **49**, 2486-2495.

17. Y. Seo, Y. S. Cho, Y. D. Huh and H. Park, Copper ion from Cu_2O crystal induces AMPK-mediated autophagy via superoxide in endothelial cells. *Mol. Cells*, 2016, **39**, 195.

18. K. H. Caffall and D. Mohnen, The structure, function, and biosynthesis of plant cell wall pectic polysaccharides, *Carbohyd. Res.*, 2009, **344**, 1879-1900.

19. H. Zhong and A. Läuchli, Changes of cell wall composition and polymer size in primary roots of cotton seedlings under high salinity, *J. Exp. Bot.*, 1993, **44**, 773-778.

20. Y. Rui, P. Zhang, Y. Zhang, Y. Ma, X. He, X. Gui, Y. Li, J. Zhang, L. Zheng, S. Chu, Z. Guo, Z. Chai, Y. Zhao, and Z. Zhang, Transformation of ceria

nanoparticles in cucumber plants is influenced by phosphate, *Environ. Pollut.*, 2015, **198**, 8-14.

21. B. Ravel and M. Newville, ATHENA, ARTEMIS, HEPHAESTUS: data analysis for X-ray absorption spectroscopy using IFEFFIT, *J. Synchrotron Radiat.*, 2005, **12**, 537-541.

22. S. Zhang, Y. Jiang, C. S. Chen, D. Creeley, K. A. Schwehr, A. Quigg, W. C. Chin and P. H. Santschi, Ameliorating effects of extracellular polymeric substances excreted by *Thalassiosira pseudonana* on algal toxicity of CdSe quantum dots, *Aquat. Toxicol.*, 2013, **126**, 214-223.

23. N. Blumenkrantz and G. Asboe-Hansen, New method for quantitative determination of uronic acids, *Anal. Biochem.*, 1973, **54**, 484-489.

24. S. Eda, K. Miyabe, Y. Akiyama, A. Ohnishi and K. Katö, A pectic polysaccharide from cell walls of tobacco (*Nicotiana tabacum*) mesophyll, *Carbohyd. Res.*, 1986, **158**, 205-216.

25. R. R. Selvendran and M. A. O'Neill, Isolation and analysis of cell walls from plant material, *Methods of biochemical analysis*, 1987, 25-153.

26. A. C. Olson, Proteins and plant cell walls. Proline to hydroxyproline in tobacco suspension cultures, *Plant Physiol.*, 1964, **39**, 544-550.

27. J. F. Shepard and R. E. Totten, Isolation and regeneration of tobacco mesophyll cell protoplasts under low osmotic conditions, *Plant Physiol.*, 1975, **55**, 689-694.

28. M. B. Sheahan, D. W. McCurdy and R. J. Rose, Mitochondria as a connected population: ensuring continuity of the mitochondrial genome during plant cell

dedifferentiation through massive mitochondrial fusion, *Plant J.*, 2005, **44**, 744-755.

29. M. Gonzalezdavila, J. M. Santanacasiano, J. Perezpena and F. J. Millero, Binding of Cu(II) to the surface and exudates of the alga *Dunaliella tertiolecta* in seawater, *Environ. Sci. Technol.*, 1995, **29**, 289-301.

30. A. J. Miao, K. A. Schwehr, C. Xu, S. J. Zhang, Z. Luo, A. Quigg and P. H. Santschi, The algal toxicity of silver engineered nanoparticles and detoxification by exopolymeric substances, *Environ. Pollut.*, 2009, **157**, 3034-3041.

31. L. Wu, L. K. Tsui, N. Swami and G. Zangari, Photoelectrochemical stability of electrodeposited Cu_2O films, *J. Phys. Chem. C.*, 2010, **114**, 11551-11556.

32. A. Synytsya, M. Urbanová, V. Setnička, M. Tkadlecová, J. Havlíček, I. Raich, P. Matějka, A. Synytsya, J. Čopíková and K. Volka, The complexation of metal cations by D-galacturonic acid: a spectroscopic study, *Carbohyd. Res.*, 2004, **339**, 2391-2405.

33. C. Ramesh, M. HariPrasad and V. Ragunathan, Effect of *Arachis hypogaea* L. leaf extract on Barfoed's solution; Green synthesis of Cu_2O nanoparticles and its antibacterial effect, *Curr. Nanosci.*, 2011, **7**, 995-999.

34. I. Prakash, P. Muralidharan, N. Nallamuthu, M. Venkateswarlu and N. Satyanarayana, Preparation and characterization of nanocrystallite size cuprous oxide, *Mater. Res. Bull.*, 2007, **42**, 1619-1624.

35. S. Deiana, C. Gessa, V. Solinas, P. Piu and R. Seeber, Complexing and redox properties of the system D-galacturonic acid-iron (III), *J. Inorg. Biochem.*, 1989,

35, 107-113.

36. S. Panigrahi, S. Kundu, S. Ghosh, S. Nath and T. Pal, General method of synthesis for metal nanoparticles, *J. Nanopart. Res.*, 2004, **6**, 411-414.

37. M. Branca, G. Micera and A. Dessí, Reduction of chromium (VI) by D-galacturonic acid and formation of stable chromium (V) intermediates, *Inorg. Chim. Acta.*, 1988, **153**, 61-65.

38. R. Ma, J. Stegemeier, C. Levard, J. Dale, C. Noack, T. Yang, Jr. G. E. Brown and G. V. Lowry, Sulfidation of copper oxide nanoparticles and properties of resulting copper sulfide, *Environ. Sci.: Nano*, 2014, **1**, 347-357.

39. D. Q. Zhang, H. J. Zeng, L. Zhang, P. Liu and L. X. Gao, Influence of oxygen and oxidant on corrosion inhibition of cysteine self-assembled membranes for copper, *Colloids and Surfaces A.*, 2014, **445**, 105-110.

40. A. Manceau, K. L. Nagy, M. A. Marcus, M. Lanson, N. Geoffroy, T. Jacquet and T. Kirpichtchikova, Formation of metallic copper nanoparticles at the soil - root interface, *Environ. Sci. Technol.*, 2008, **42**, 1766-1772.

41. S. Y. Ding, Y. S. Liu, Y. Zeng, M. E. Himmel, J. O. Baker and E. A. Bayer, How does plant cell wall nanoscale architecture correlate with enzymatic digestibility? *Science*, 2012, **338**, 1055-1060.

42. G. Noctor, R. De Paepe and C. H. Foyer, Mitochondrial redox biology and homeostasis in plants, *Trends plant sci.*, 2007, **12**, 125-134.

43. J. G. Mesu, A. M. Beale, F. M. de Groot and B. M. Weckhuysen, Probing the influence of X-rays on aqueous copper solutions using time-resolved in situ

combined video/X-ray absorption near-edge/ultraviolet-visible spectroscopy, *J. Phys. Chem. B.*, 2006, **110**, 17671-17677.

44. M. Pilon, Moving copper in plants, *New Phytol.*, 2011, **192**, 305-307.

45. U. Ndon, A. Randall and T. Khouri, Reductive dechlorination of tetrachloroethylene by soil sulfate-reducing microbes under various electron donor conditions, *Environ. Monit. Assess*, 2000, **60**, 329-336.

Figures and Tables
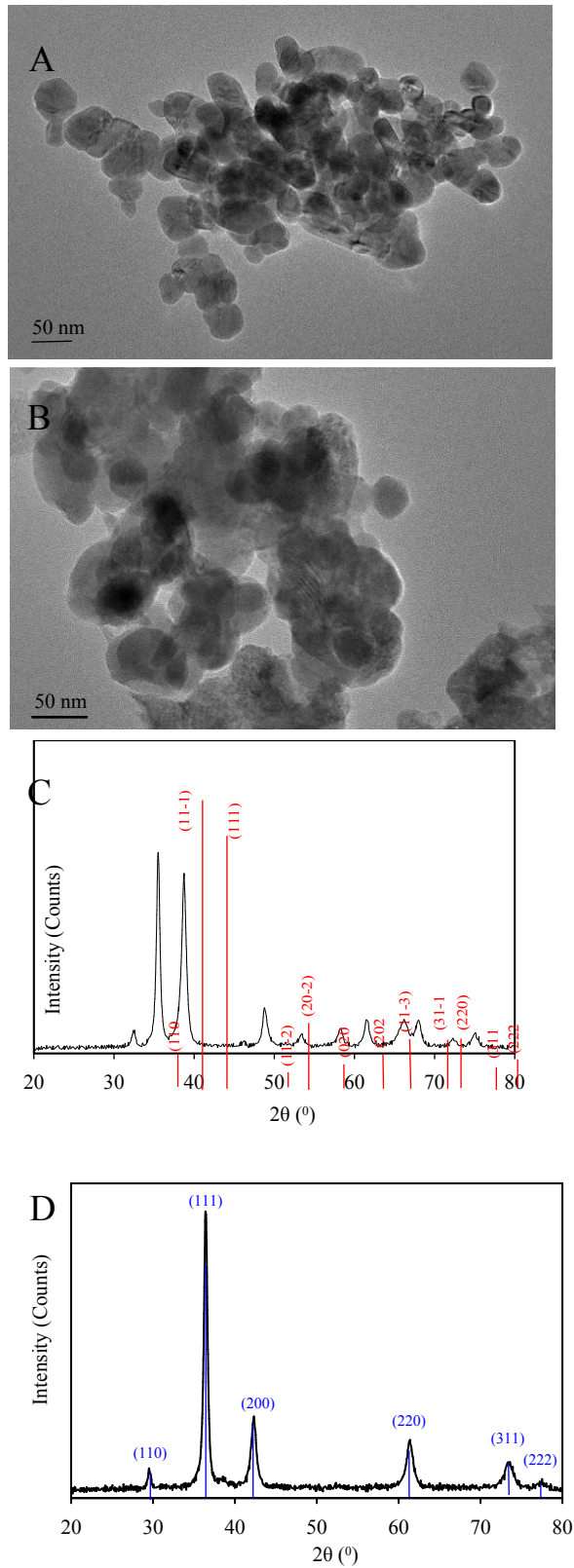
Figure 1. TEM and XRD images of NPs. Images (A) and (B) are TEM images of CuO

NPs and Cu$_2$O NPs, respectively. Images (C) and (D) are XRD spectra of CuO NPs

and Cu$_2$O NPs, respectively. The peaks corresponding to red/blue lines suggest CuO/Cu$_2$O crystal planes.
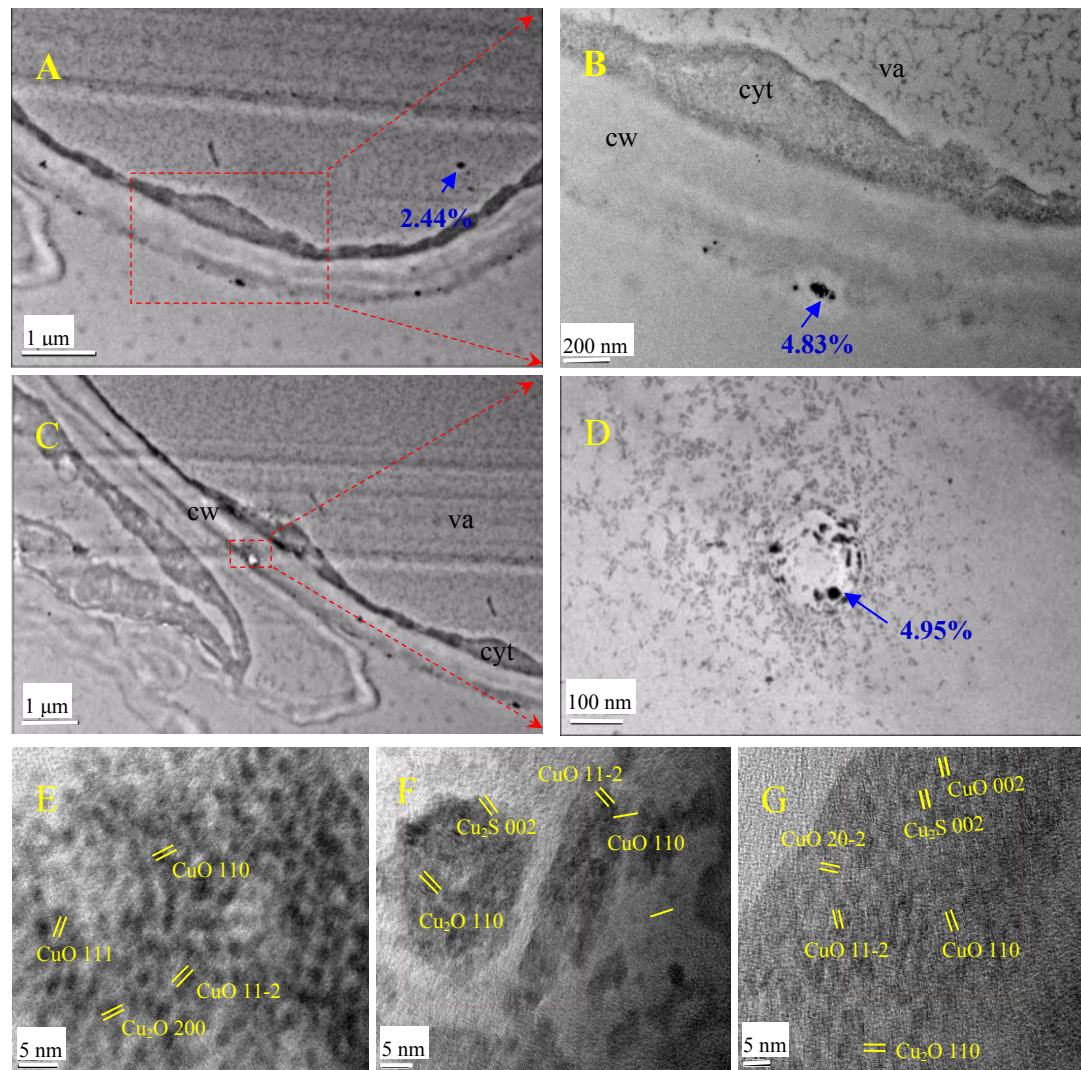
Figure 2. TEM images of cells after exposure to CuO NPs (12 mg/L) for 12 h. Images (B) and (D) are the enlarged images from (A) and (C), respectively. (E), (F): HRTEM images of black points indicated by blue arrows in (B) and (D), respectively. Image G is HRTEM of particles in (A) marked with blue arrows. Black points are analyzed by EDS, and the weight percentages of Cu are listed around the black particles in the TEM images (marked with blue arrows). cw: cell wall; cyt: cytoplasm; va: vacuole.
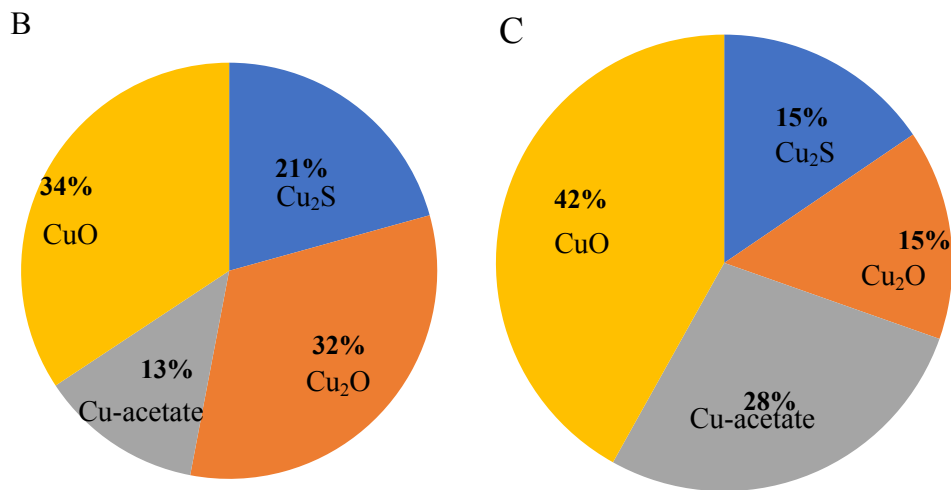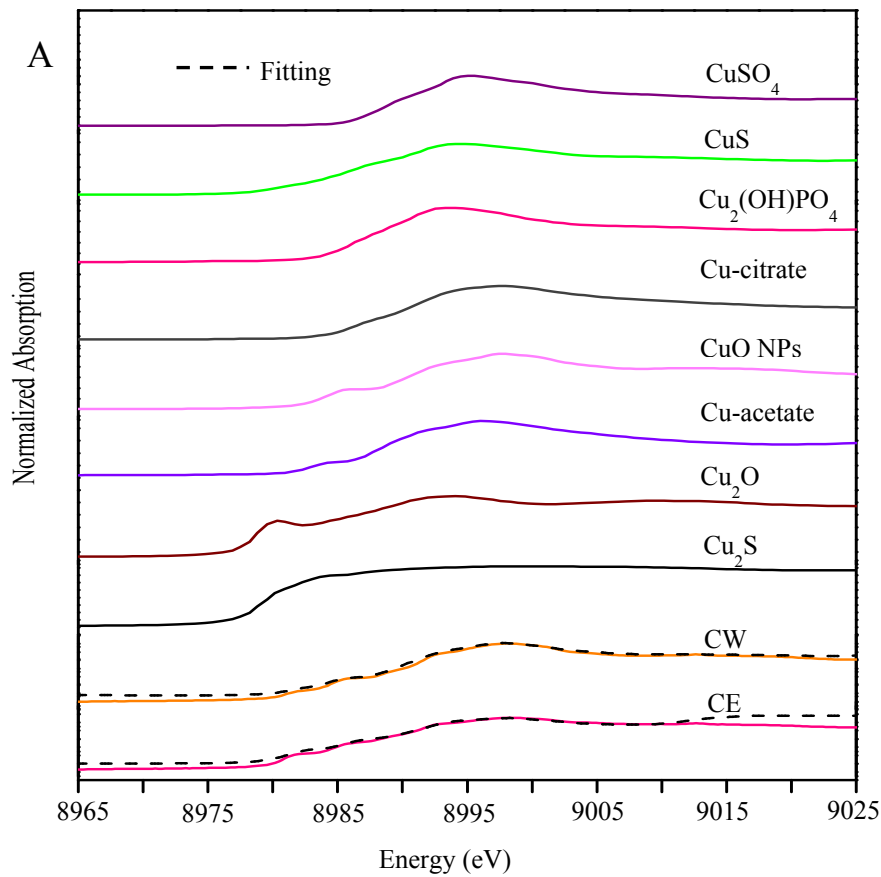
Figure 3. Cu species in the "CuO NP-exposed cells" and "cell walls extracted from CuO NP-exposed cells" as identified by XANES. (A): The XANES curves of Cu species in the whole cells and cell walls. In panel (A), the black dashed line is the fitting curve. (B), (C): the percentages of Cu components in cells and extracted cell

walls. CE is the cells exposed to CuO NPs (12 mg/L) for 12 h. CW is the cell walls

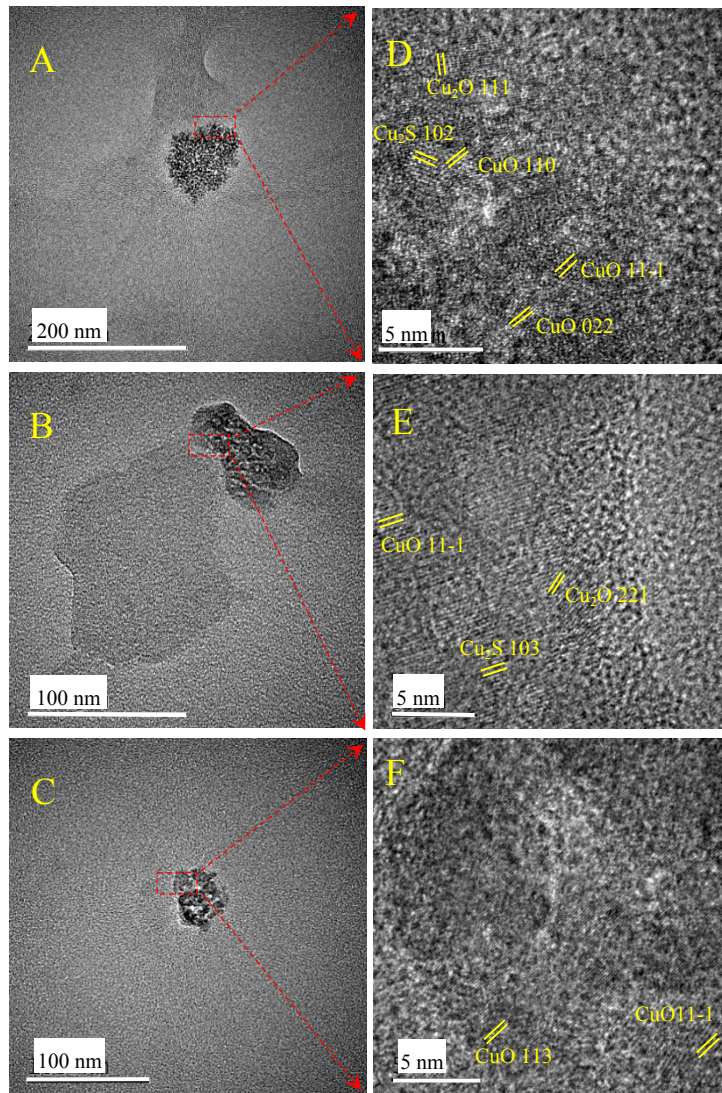extracted from cells under the exposure of CuO NPs (12 mg/L) for 12 h.

Figure 4. TEM images of cell walls and EPS after incubation with CuO NPs. (A): Cell walls extracted from un-exposed cells, and then incubated with CuO NPs (12 mg/L) for 12 h. (B): Cell walls extracted from cells under exposure of CuO NPs (12 mg/L, 12 h). (C): EPS exposed to CuO NPs. Cells cultured for 3 days and then filtered with 18-μm stainless steel sieve. The filtrate EPS was further incubated with CuO NPs (12 mg/L) for 12 h. (D), (E), (F) are HRTEM images enlarged from (A), (B), (C) marked with red dashed boxes.
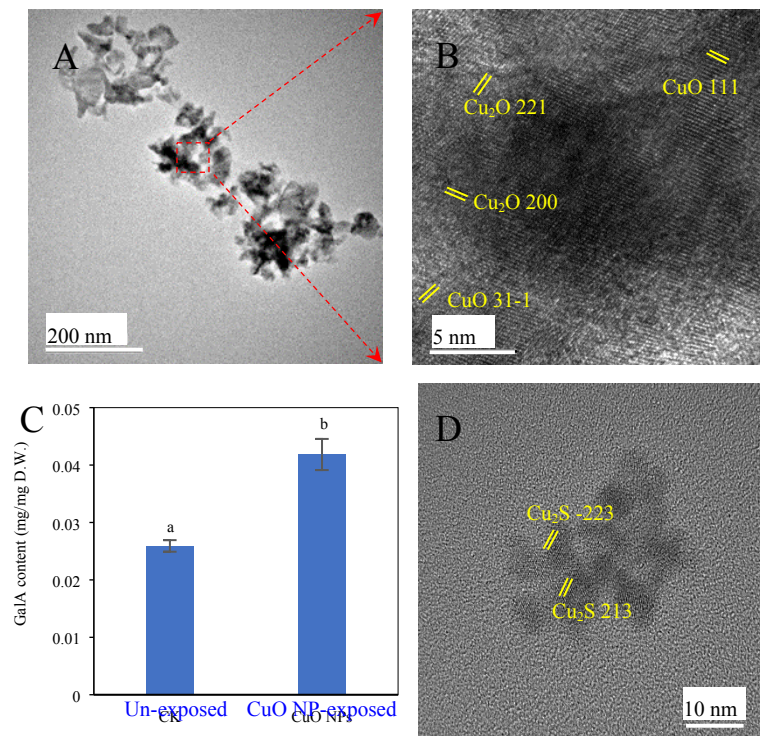
Figure 5. TEM images of CuO NPs after incubation with GlaA and L-cysteine. (A): TEM image of CuO NPs (12 mg/L) after incubation with GlaA (200 mg/L) for 12 h. (B): HRTEM image of GlaA-treated CuO NPs enlarged from (A) (marked with red dashed box). (C): Intracellular GlaA content of cell walls under exposure of CuO NPs (12 mg/L) for 12 h. (D): HRTEM image of L-cysteine (9 mg/L) treated CuO NPs (12 mg/L) over 12 h. The crystal spacings of CuO (31-1) and (111) are 0.141 and 0.233 nm, respectively. The crystal spacings of 0.218 and 0.143 nm correspond to Cu_2O (200) and (221), respectively. The crystal spacings of Cu_2S (-223) and (213) are 0.355 and 0.288 nm, respectively. D. W.: cell wall dry weight.
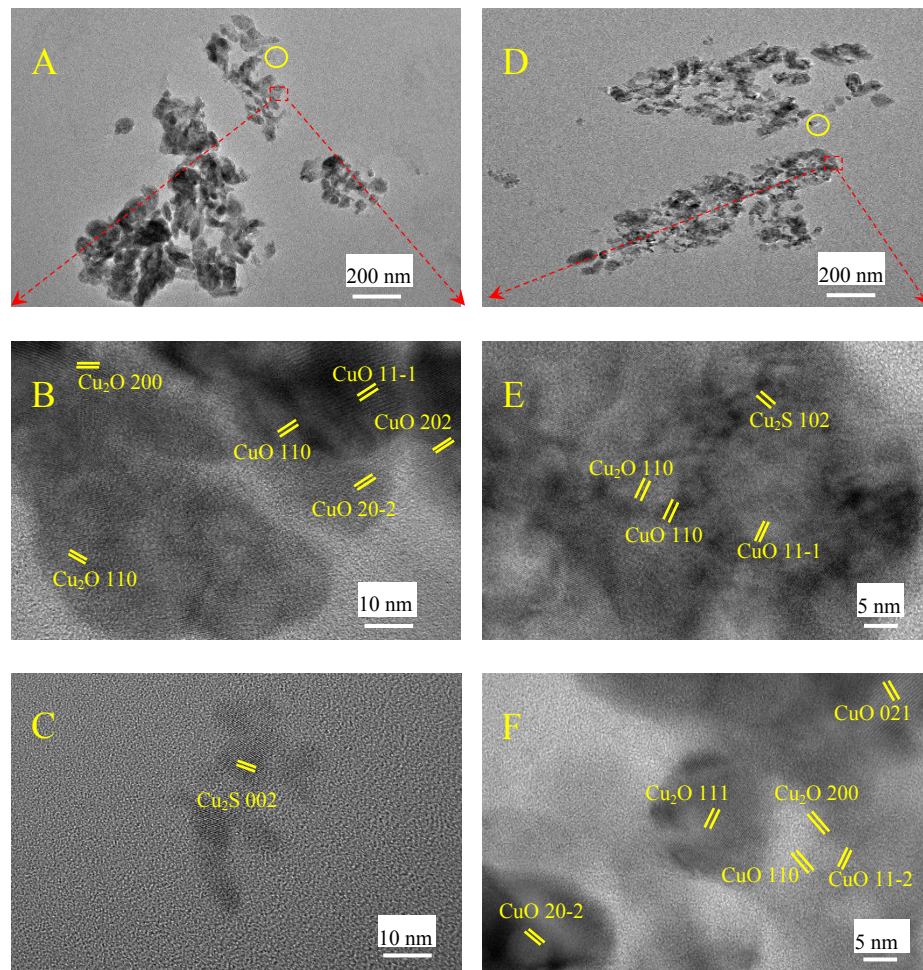
Figure 6. TEM images of CuO NPs after exposure to protoplasts and mitochondria extracted from un-exposed cells. (A), (D): TEM images of CuO NPs (12 mg/L) exposed to protoplast and mitochondria for 12 h, respectively. (B), (E): HRTEM images enlarged from (A) and (D) that are marked with red dashed boxes. Images (C) and (F) are HRTEM images enlarged from (A) and (D) as marked with yellow circles, respectively.

Graphic Abstract
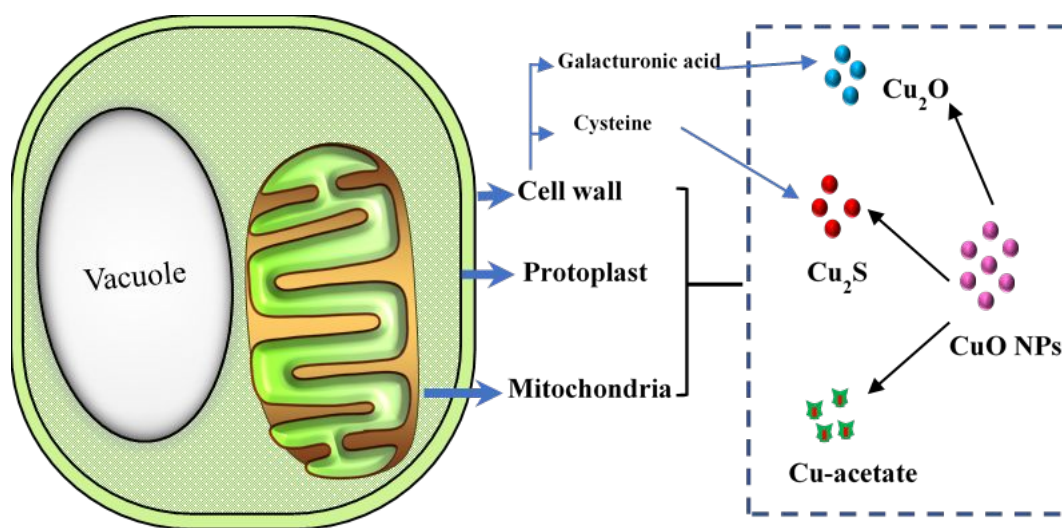
CuO NPs were transformed to Cu_2O, Cu_2S, and Cu-acetate on the cell walls and

inside plant cells.